SLAC-PUB-11131
April 2005

Measurements of Coherent Cherenkov Radiation in Rock Salt: Implications for GZK Neutrino Underground Detector

R. Milincic, P. W. Gorham, and E. Guillian
Dept. of Physics & Astronomy, Univ. of Hawaii at Manoa, 2505 Correa Rd. Honolulu, HI, 96822
D. Saltzberg and D. Williams
Dept. of Physics & Astronomy, Univ. of Calif. at Los Angeles, Los Angeles, CA
R. C. Field and D. Walz
Stanford Linear Accelerator Center, Stanford University, Menlo Park California

We present results of the study of coherent Čerenkov radiation from negative charge excess in electromagnetic cascades (Askaryan effect) in synthetic rock salt. In the first part of this work, the accelerator measurement was performed in the Stanford Linear Accelerator with pulsed bunches of 28.5 GeV electrons passing through Aluminum radiators, which produced a beam of bremsstrahlung photons in direction of the salt. Measurements cover the range of shower energies from $2.7 \times 10^{14} eV$ up to $8.0 \times 10^{18} eV$. With three different types of radio frequency receivers which altogether span the range of 200 - 20000 MHz, we analyzed coherency of radiation produced within the target salt. In the second part, we conducted a search for the coherent radio pulses induced by high energy cosmic-rays. As a medium for detection of Čerenkov radiation, we use a 22 ton target of synthetic rock salt contained within a scintillation counter cosmic-ray hodoscope. Two parallel arrays of crossed bowtie antennas are put inside the salt bed and used as a detection tool. Here, we present expected rate for detection of cosmic ray protons and secondary muons above 'Salt Factory' sensitivity of 1.8 TeV. These measurements provide an excellent baseline for the Monte Carlo simulation of the performance of the 15.6 km^3 GZK neutrino detector placed inside a salt-dome formation. Results of the simulations show that this kind of detector can be used to put constraints on all GZK neutrino models in one year of work.

1. Introduction

The main messengers of the processes in the deep universe, arriving to us, are protons, photons and neutrinos. Unfortunately, if the distance from a source is greater than 50-100 mega parsecs, high energy photons will interact with the 2.7 K photons of Cosmic Microwave Background (CMB) [1] before reaching detectors on the Earth. The same fate awaits high energy protons whose spectrum suddenly drops after $19.5 \times 10^{19} eV$ (Greisen, and Zatsepin & Kuzmin (GZK) cut off [2, 3]).

Hence, only neutrinos are capable of passing great distances (due to their extremely weak interaction with matter) carrying the information about the moments as far back in time as just after the Big Bang. However, the expected flux of ultra high energy neutrinos requires detectors with target volume of the order of magnitude 10^{42} nucleons [4]. So far, the most promising approach to extract information about GZK neutrinos from these huge mass detectors is by utilizing the Askaryan effect [5]. Ice, as a target material, has already been employed on Antarctic, where the Radio Ice Cerenkov Experiment (RICE) [6] has been operating for several years. Besides, there is also a new promising experiment - the Antarctic Impulsive Transient Antenna (ANITA) [7] expecting results in 2007.

Our approach is to use a huge rock salt formation as a target medium (first suggested by Askaryan [5]) for GZK neutrino detection via Askaryan effect. Viability of this approach is verified with accelerator measurement of the Askaryan process in rock salt in the energy range of interest for GZK neutrino detection (done in June 2002), and also with the 'Salt factory' detector of Cosmic rays. Thus, these results open the road to Teraton neutrino detectors.

2. Accelerator Measurement of the Askaryan effect in Rock Salt

The experimental setup is shown in Fig. 1. Rock salt, used in the experiment was in the form of trapezoid bricks with middle line dimensions of $15 \times 10 \times 6$ cm, with a single brick mass of 1.8 kg and manufactured claimed purity of 99.5%. Attenuation length is a couple of hundred meters [11] in the UHF regime for the used frequency range. All together, almost 4 tons of sodium chloride were put in the Final Focus Test Beam (FFTB) facility at SLAC. When building the target geometry, the care was taken, so that one side of salt stack is within a 10° angle toward the beamline (done with a 2.5 cm thick polyethylene sheet) to avoid the total internal reflection of the Čerenkov radiation. Inside the salt stack and 35 cm above the beamline, in horizontal plane, an array of 21 printed-circuit board (PCB) broadband dual-linear-polarization bowtie antennas is buried. The centers of neighboring antennas are on the same axis, with the average distances of 22 cm in the direction of the beam and 21 cm in the perpendicular direction. The polarization of each antenna was carefully arranged according to the shower axis. Outside of salt and on the horizontal level of the beam, we placed a C/X-band horn and a log-periodic

Submitted to 22nd Texas Symposium on Relativistic Astrophysics at Stanford University, Stanford, California, 13-17 Dec 2004.

Work supported in part by the Department of Energy contract DE-AC02-76SF00515

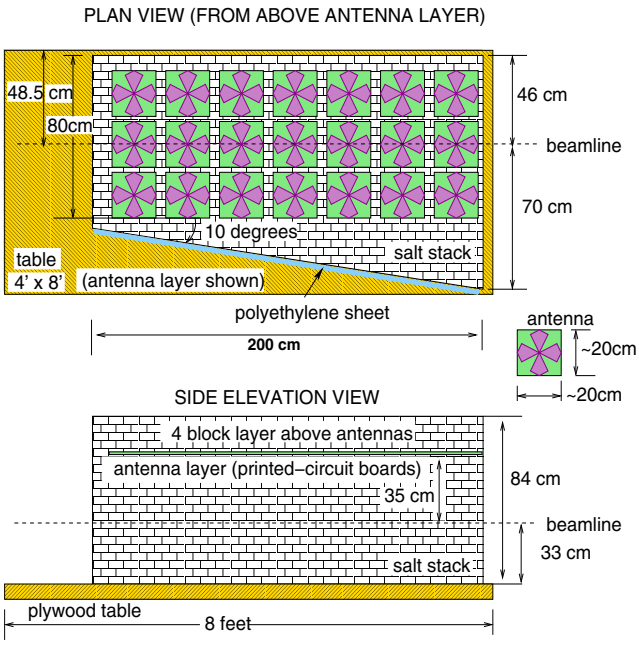

Figure 1: Experimental setup for measurement of Askaryan effect in rock salt.

dipole array (LPDA) antenna, both on the distance of 75 cm from the polyethylene wall in the direction of the expected Čerenkov radiation after its refraction from dielectric borders and positioned on the axis of the shower maximum. With these three types of antennas, covered frequency range is 0.2-18 GHz, where bowtie antennas have good response in the range 0.2-2 GHz, horn has good response in the frequency range from 5 to 9 GHz and LPDA 1-18 GHz. Data collection is done with two oscilloscopes, TDS694C for low and CSA8000 for high frequency. Trigger was issued from a microwave transition-radiation receiver, located upstream.

Beam of 28.5 GeV electrons was directed toward the bremsstrahlung radiators located in front of the main salt target at 3 m distance from it. Like in our previous SLAC measurement [10], as a radiator for production of bremsstrahlung gamma-rays, we used Aluminum of different thickness from 0.06% to 1.5% of a radiation length. The direction of electrons passing through the radiators was changed in such a way that electrons do not enter and initiate showers in the salt target. By combining different thickness of available radiators and changing the electron flux in the beam, we were able to span measurements over 4 orders of magnitude in shower energy. The measurements were performed by averaging 1000 triggers and after that 100-1000 single shot triggers to monitor stability.

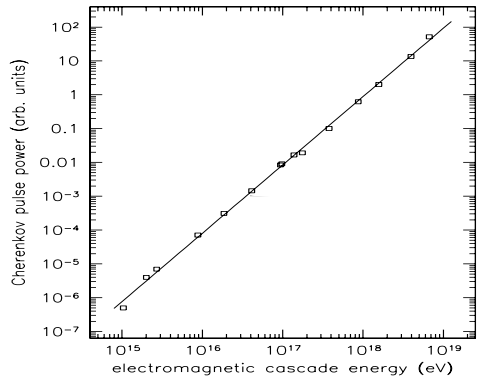

Figure 2: Time domain measurement of coherence obtained with printed-circuit board broadband (0.3-1.5GHz) dual-linear-polarization bowtie antennas. The curve is a fit which shows a quadratic dependence of power from shower energy.

2.1. Characteristics of Measured Electric Field

The bands of antennas provide us with the opportunity to measure coherency of different parts of the Čerenkov radiation spectrum. For the frequency below the frequency of decoherency $\nu_0 = 2700MHz$ (estimation for rock salt as a medium), we used bowtie antennas which are positioned around the shower maximum. With the distance between the beam and antenna in the direction of the Čerenkov angle $R = 38$ cm, the largest antenna dimension $L = 20$ cm, and the angle $\theta = 25°$ toward antenna axis and for the antenna bandwidth, conditions for far field approximation are satisfied. Fig. 2 shows the results of the measurements of the relative radio-frequency power as a function of shower energy. Here, we extend the energy range up to $8.0 \times 10^{18}eV$ and go as low as $2.7 \times 10^{14}eV$ which can be compared to [10]. We do not observe any deviation from quadratic increase of pulse power with shower energy. For an accurate calculation of electric field strength received by antennas, it is required that the antenna effective area, spectral response, coupling efficiency, angular response and, also in the case of shower induced field a finite spatial region over which a pulse is formed coherently (so called coherence zone, which is a function of frequency), all be included in converting the measured voltages to field strengths. For determining the coherence at higher frequencies (2.2-15.0 GHz), around and above ν_0 we use the LPDA and the C/X-band horn antennas, both of which had known effective areas and antenna factors. Fig. 3 shows the measured electric field strength vs. total shower energy at three different frequencies. Measurements were done with the LPDA on 4.95 and 14.5 GHz, respectively, and with the horn antenna at 7.4 GHz. Points represent mea-

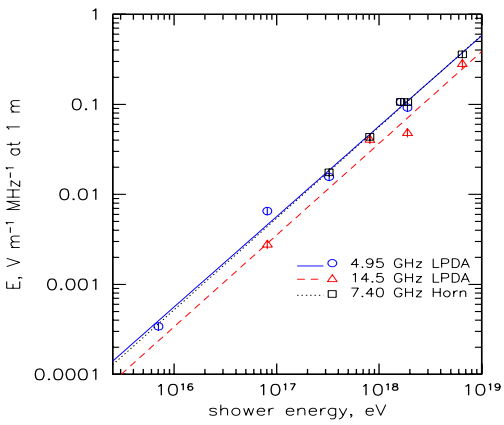

Figure 3: Measured electric field strength at 4.95, 14.5 with LPDA and 7.4 GHz with horn antennas respectively, together with the least-square fit curves. It indicates that coherency of RF signal in rock salt extends to almost 15 GHz.

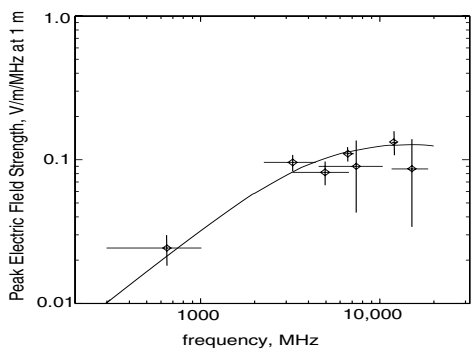

Figure 4: Spectrum of the measured electric field strength for shower energy $1.9 \times 10^{18} eV$. The curve is ZHS parameterization in rock salt.

sured values and lines are the least-square fit curves $|\mathbf{E}| = A{E_{sh}}^{\alpha}$, where $\mathbf{E}$ is the electric field and E_{sh} the shower energy. The fit for the exponent α gives: $\alpha_{4.95} = 1.00 \pm 0.04$ at 4.95 GHz, $\alpha_{14.5} = 1.02 \pm 0.11$ at 14.5 GHz, $\alpha_{7.4} = 0.99 \pm 0.05$ at 7.4 GHz. The value of α on all three frequencies indicates that the field strength is in agreement with the full coherence of radiation. Measurement of spectral dependence of the absolute field strength is shown in Fig. 4. It is done with the use of all antennas and few filters in several frequency bands from 0.3-15.0 GHz. Horizontal bars define bandwidth of antennas or filters. Plotted curve is based on the parameterization given in [13], scaled from ice to synthetic rock salt. The spectral profile of the coherent Čerenkov radiation is in good agreement with the expectation up to the highest measured frequency, where the significant variation of the field as a consequence of decoherence caused by the

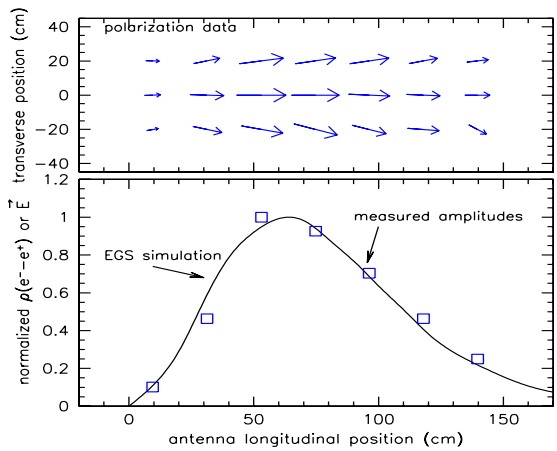

Figure 5: Top: Orientation and relative amplitude of the electric field vector measured with the bowtie antenna. Bottom: The normalized amplitude of the received RF pulses along the center line of the antenna array. Curve is a normalized EGS simulation of showers induced with bremsstrahlung photons.

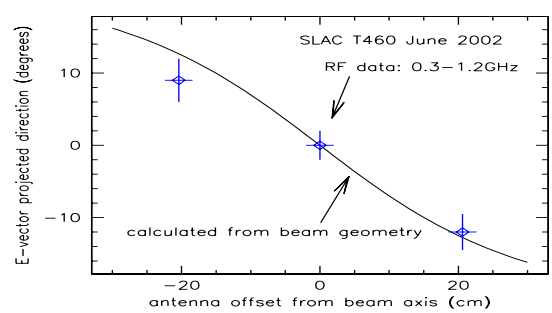

Figure 6: Angle of plane of polarization of the electric field at transverse distance of the antennas to beam vertical plane, (35 cm above the axis of the beam). Curve shows the expected angle of projected field of the Čerenkov radiation on the plane of the array.

shower profile can be seen. We also analyze the polarization characteristics of the received signal that was done with the crossed bowtie antennas (their geometry is adapted for simultaneous measurement of orthogonal linear polarization). Cross-talk between a co-polarized and the cross-polarized antennas from the same strip is measured to be 15%. In order to estimate the angle of projected plane of polarization, it is necessary to determine the part of signal received directly or as an inherent leakage on each antenna.

$$\begin{pmatrix} V_0 \\ V_{90} \end{pmatrix} = \begin{pmatrix} cos\Psi & \alpha sin\Psi \\ \alpha cos\Psi & sin\Psi \end{pmatrix} \begin{pmatrix} E \cdot h_0 \\ E \cdot h_{90} \end{pmatrix}$$

The vector effective height is $|h| = |h_0| = |h_{90}|$ from symmetry of receiving system, Ψ is projection of po-

larization angle on the plane of antenna array. Middle line of antennas is directly above and parallel with the beam axis, and they provide accurate estimate of α,($\alpha = (V_{90}/V_0)|_{on-axis}$). Thus, the measured value of Ψ is:

$$\Psi = -\tan^{-1}\left(\frac{\alpha - V_{90}/V_0}{\alpha V_{90}/V_0 - 1}\right) . \quad (1)$$

Fig. 5 shows results of the polarization and relative amplitude measurements for all bowtie antennas. The top pane plots these as vectors with scaled lengths and directions corresponding to the square root of the amplitude and the projected plane of the polarization Ψ. In the lower pane of the figure, the normalized relative amplitude of the electric field measured with the antennas along the center axis as a function of the longitudinal distance along the shower (corrected for the Čerenkov angle projection) is displayed. We also plot the EGS4 simulation of the longitudinal development of the charge excess along the shower. There is an excellent agreement between the measured shape of the amplitude response and the normalized charge excess predictions from EGS4. Figure 6 shows data for three antennas facing the shower maximum in the direction of the Čerenkov angle, plotting the plane of polarization as a function of the transverse position of the antenna with respect to the beam vertical plane in longitudinal direction. The solid curve shows the expected change of projection of the angle of polarization of the Čerenkov radiation on the antenna plane. From these results it is clear that radiation is linearly polarized and it is lying in the plane of beam line and Čerenkov radiation.

3. Salt Factory

After establishing characteristics of the RF radiation in rock salt with accelerator beam, our next goal is to make the first measurement of the coherent Čerenkov radiation from natural origin - cosmic rays induced cascade. Fig. 7 presents apparatus of the test-bed experiment placed at Manoa campus of University of Hawaii. As a detection media for the radio waves we used 22000 kg of salt in the form of blocks weighing 22.68 kg each. The purity of the salt was between 93.0% and 96.0%. Interior walls of the rectangular wooden box with dimensions 12.0 x 1.2 x 0.8 m were covered with zinc plated steel metal sheets (thickness 0.5 mm). By making this Faraday cavity, we achieved good noise reduction inside the box. Cavity was filled with salt and 22.0 cm above the bottom of the cavity, two arrays of antennas were installed. Basic element of the arrays is the same (PCB) broadband dual-linear-polarization bowtie antenna as one used in SLAC experiment. Bowtie antennas are oriented 45° toward the axis of each array and placed

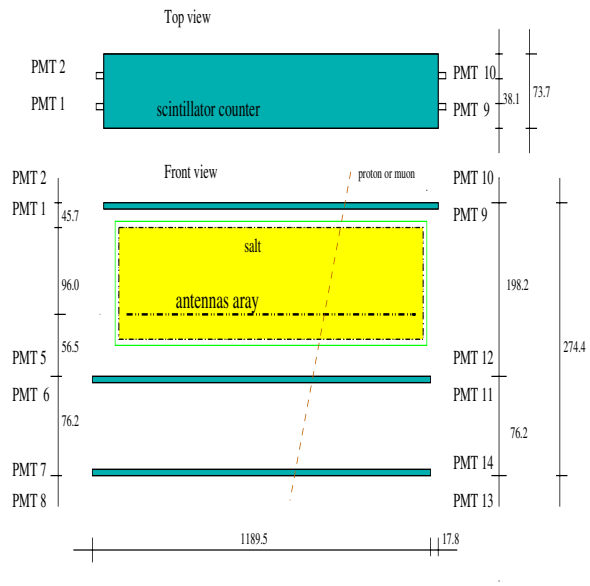

Figure 7: Experimental setup for the Salt factory.

27.0 cm apart. There are 48 bowties in every line and linear distance between each two antennas in one array is 25.0 cm. Due to the limited number of digitizing channels, we had to combine signals from four antennas with the same polarization orientation into one channel, and a 4 to 1 hybrid combiner is used to accomplish this.

The trigger system for the test-bed experiment is based on macro counters: twelve 12"(30.5 cm diameter) photomultiplier tubes (PMTs) were distributed in three layers. The top layer was 142 cm above antenna level while the middle PMT layer was 57 cm and bottom PMT layer was 133 cm below the antenna's layer. Together, they formed one trigger system. Every layer consisted of 12 m long, 0.7 m wide and 0.3 m high liquid scintillator filled box. Two PMTs were placed on each end of liquid scintillator box, facing the scintillator. The threshold voltages for PMT signals were defined separately for each detector layer, and they were set to the PMT pulse height that corresponds to the muon energy of ∼100GeV.

3.1. Analysis

Characteristics of the 4 to 1 hybrid signal was tested in the SLAC Final Focus Test Beam facility and result is shown in the Fig. 8. It presents polarization analysis of the ratio of the pulses recorded by parallel and normally oriented parts of the crossed bowtie antennas. The result shows that information about polarization characteristics of the radiation is contained within the signal and justifies such a coupling. This provides a solid baseline for calibration of the test-bed detector capabilities. In addition, measurement of the

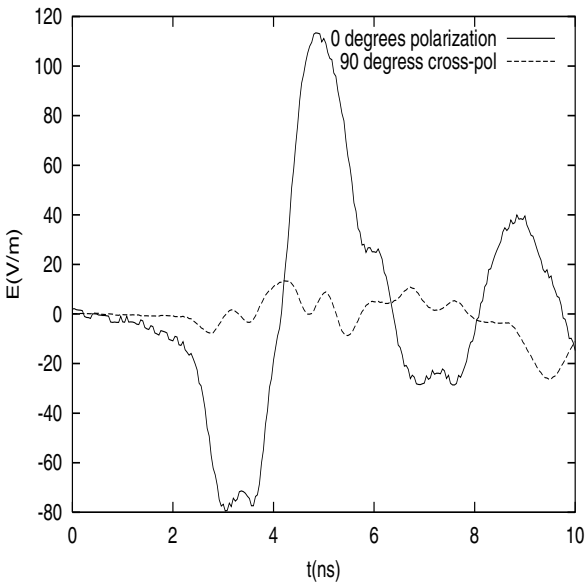

Figure 8: The averaged polarization and amplitude of pulse received by 4 in 1 hybrid combiner, from bowtie antennas.

electronic component of the system provides 1.8 MeV threshold energy for the 1σ effect. Fig. 9 shows the simulation of the expected event rate from the primary CR protons and the secondary muons per year at 1σ SNR, to be about 12 events. However, variation

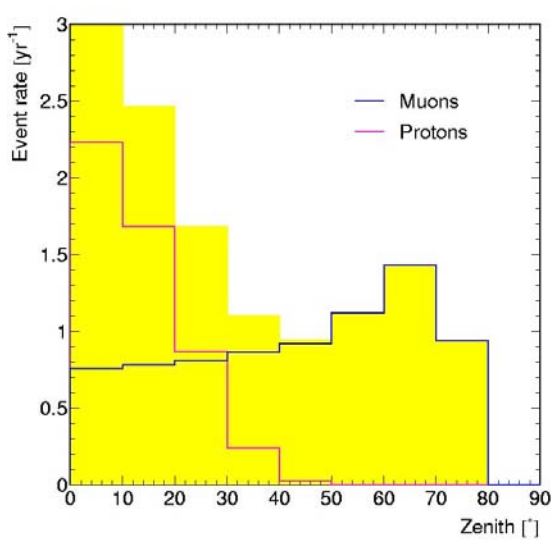

Figure 9: Monte Carlo simulation of the expected event rate per angle in the salt detector.

in noise caused with significant RF pollution and its unpredictability indicates that 2σ SNR signal, at the level which can be confidently confirmed, gives us the event rate of 1.4 events per year. Single event analysis of the first two months of data, did not show any candidates that passed all analysis cuts.

4. Salt dome Shower Array (SalSA)

Results of the measurements demonstrate that Askaryan effect in rock salt can be used to precisely reconstruct shower development and the total shower energy. The polarization properties of the produced coherent Čerenkov radiation give excellent reconstruction of primary particles tracks. Together with the measurement of attenuation of RF signal in salt domes [9] which indicates $\geq$ 250 m attenuation length, our results show that very large salt structures can successfully be used for GZK neutrino detection. Luckily, geological history of our planet is such, that all around the world, hundreds of huge (tens of km^3 in size) compact formations of salt exist with purity as high as 98.0% -99.0%. These huge salt dome formations can relatively easily be utilized for the development of detectors for ultra-high energy particles, particularly neutrinos with energies around GZK cutoff.

We have created a Monte Carlo simulation of a large-scale antenna array embedded in a salt dome as described above. In the first approximation we assumed cube geometry (in reality, detector geometry will be optimized for the Čerenkov angle in salt and for the angular distribution of probability of detection for different neutrino flavors), with 1728 antenna nodes for whole detector, with a grid spacing of 225 m, based on estimates [9] of the attenuation length in rock salt. The volume of complete detector is taken to be just above 15 km^3 and together with the volume enclosing one attenuation length around it, increases to 25km^3 which is 137 km^3 of water mass equivalent.

Each node consists of 6 RICE type dipoles with linear polarization oriented vertically, 6 slotted-cylinder antennas with horizontal polarization and 0.75 m between each two consecutive antennas. The pattern and frequency response of these antennas are well known [14]. Antennas are optimized for frequencies centered at about 200 MHz, with bandwidth of 100-300 MHz. We require that signal must be above 2.8σ on 5 out of 12 node cell antennas in order to trigger the system and collect data. This kind of triggering scheme will significantly reduce triggering from any background noise.

The 225 m spacing will give shower energy threshold slightly above 30 PeV for $L_\alpha = 250$ m, but sensitivity to energies around 100 PeV, can be expected more realistically, because of the contribution of additional losses and uncertainties of interactions at these energies. These shower energies are in the range of the GZK neutrino spectrum peak $\sim$ 100 PeV.

It was also assumed that neutrino flavors are completely mixed with ratio of 1:1:1 $= \nu_e : \nu_\mu : \nu_\tau$ (average

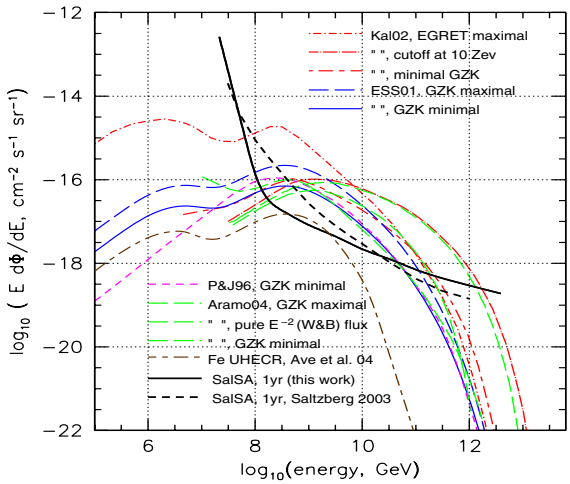

Figure 10: Estimated sensitivity for SalSA for one year of exposure. A set of GZK models is shown, as well as an earlier estimate of SalSA sensitivity [19].

distance to source is longer than oscillation length), flux is isotropic on the Earth surface and monoenergetic at discrete energies in $10^{15}eV - 10^{2}1eV$ range. Estimates of the power of the radio emission is based on the Zas-Alvarez-Muñiz parameterization [13] with implementation of differences between ice and salt.

Fig. 10 shows the results of simulation for 1 year of full operation of SalSA detector together with the expectation based on previous SalSA estimate (without node cells) [19]. The plot also compares several classes of models of GZK neutrino fluxes [16–18] with SalSA. With 1 year of exposure SalSA will be able to put constraints even for the most conservative prediction (expected rate is 11-14 events), and in the case that the optimistic models are to take place, the number of events can rise above 100 events/year. Nature of detector gives an opportunity for a long operating life, which can collect huge amounts of data, enough to characterize GZK neutrinos as an important piece for solving mystery of the early universe. The dimensions of the salt dome together with already existing technology for drilling deep holes (developed for oil industry), give opportunity to build even larger detectors for further exploration of GZK neutrino spectrum.

Acknowledgments

We thank the staff of the Experimental Facilities Division at SLAC for their support of our efforts, M. Rosen at the Univ. of Hawaii; D. Besson, J. Learned, A. Odian, and W. Nelson for advice and useful discussion. This work was performed in part at the SLAC, under contract with the US Dept. of Energy, and at UCLA under DOE contract DE-FG03-91ER40662, and under DOE contract DE-FG03-94ER40833 at the University of Hawaii.

References

[1] F. Halzen *et al*, Phys. Rev. D 4, 342 (1990); J. Wdowczyk & A. W. Wolfendale, Ap. J. 349, 35 (1990).
[2] K. Greisen , 1966, Phys. Rev. Lett., **16**, 748.
[3] G. T. Zatsepin & V. A. Kuzmin, Pis'ma Zh. Eksp. Teor. Fiz. 4 (1966) 114 [JETP. Lett. 4 (1966) 78]. Sov. J. Nucl. Phys. 11, 111 (1970);
[4] D. Seckel & G. Frichter, Proc. 1st Int. Workshop Rad. Detect. High Energy Part. (RADHEP 2000), ed. Saltzberg & Gorham , (AIP press) (2001).
[5] G. A. Askaryan,1962, JETP 14, 441
[6] I. Kravchenko et al., Astropart.Phys. 20 (2003) 195-213.
[7] A. Silvestri,*et al*, (2004) astro-ph/0411007
[8] M. Chiba *et al*, (2004) Phys. Atom. Nuclei 67(11), 2050.
[9] P. Gorham *et al*, NIM A490, 476, (2002).
[10] D. Saltzberg, P. Gorham, D. Walz,*et al*, 2001, Phys. Rev. Lett., **86**, 2802.
[11] A. von Hippel, editor, *Dielectric Materials and Applications*, (1995 ed.), Artech House.
[12] W. R. Nelson *et al*, SLAC-265, 1985.
[13] J. Alvarez–Muñiz, & E. Zas, 1997, Phys. Lett. B, 411, 218
[14] J. D. Kraus, 1988, *Antennas*, (McGraw-Hill:New York)
[15] L. A. Anchordoqui, *et al*, Phys. Rev. D66 (2002) 103002.
[16] O. E. Kalashev *et al*, Phys. Rev. D **66**, 063004 (2002).
[17] R. J. Protheroe & P. A. Johnson, Astropart. Phys. 4 (1996) 253.
[18] C. Aramo, *et al*, 2004, Astropart. Phys., in press; astro-ph/0407638.
[19] D. Saltzberg, *et al*, (2003), Proc. SPIE conf. 4858, Part. Astroph. Instrum., P. Gorham, ed., (SPIE: Bellingham, WA), 191.
[20] E. Waxman and J. N. Bahcall,
[21] J. L. Feng & A. D. Shapere, Phys. Rev. Lett. 88, 021303 (2002); J. Alvarez-Muniz *et al*, Phys.Rev. D65 (2002) 124015.